Near-Infrared Optical Contrast of Skull Base Tumors During Endoscopic Endonasal Surgery

Jun W. Jeon, BS*
Steve S. Cho, BS*
Shayoni Nag, BA*
Love Buch, BS*
John Pierce, MS*
YouRong S. Su, MD*
Nithin D. Adappa, MD‡
James N. Palmer, MD‡
Jason G. Newman, MD§
Sunil Singhal, MD§
John Y. K. Lee, MD, MSCE*

*Department of Neurosurgery, Hospital of the University of Pennsylvania, Philadelphia, Pennsylvania; ‡Department of Otorhinolaryngology, Hospital of the University of Pennsylvania, Philadelphia, Pennsylvania; §Department of Surgery, Hospital of the University of Pennsylvania, Philadelphia, Pennsylvania

Correspondence:
John Y. K. Lee, MD, MSCE,
235 South Eight Street,
Philadelphia, PA 19106.
E-mail: leejohn@uphs.upenn.edu

Received, February 27, 2018.
Accepted, August 7, 2018.
Published Online, August 16, 2018.

BACKGROUND: Near-infrared (NIR) tumor contrast is achieved through the "second-window ICG" technique, which relies on passive accumulation of high doses of indocyanine green (ICG) in neoplasms via the enhanced permeability and retention effect.

OBJECTIVE: To report early results and potential challenges associated with the application of second-window ICG technique in endonasal endoscopic, ventral skull-base surgery, and to determine potential predictors of NIR signal-to-background ratio (SBR) using endoscopic techniques.

METHODS: Pituitary adenoma (n = 8), craniopharyngioma (n = 3), and chordoma (n = 4) patients received systemic infusions of ICG (5 mg/kg) approximately 24 h before surgery. Dual-channel endoscopy with visible light and NIR overlay were photodocumented and analyzed post hoc.

RESULTS: All tumors (adenoma, craniopharyngioma, chordoma) demonstrated NIR positivity and fluoresced with an average SBR of 3.9 ± 0.8, 4.1 ± 1.7, and 2.1 ± 0.6, respectively. Contrast-enhanced T1 signal intensity proved to be the single best predictor of observed SBR ($P = .0003$). For pituitary adenomas, the sensitivity, specificity, positive predictive value, and negative predictive value of NIR-guided identification of tumor was 100%, 20%, 71%, and 100%, respectively.

CONCLUSION: In this preliminary study of a small set of patients, we demonstrate that second-window ICG can provide NIR optical tumor contrast in 3 types of ventral skull-base tumors. Chordomas demonstrated the weakest NIR signal, suggesting limited utility in those patients. Both nonfunctional and functional pituitary adenomas appear to accumulate ICG, but utility for margin detection for the adenomas is limited by low specificity. Craniopharyngiomas with third ventricular extension appear to be a particularly promising target given the clean brain parenchyma background and strong SBR.

KEY WORDS: Brain tumor, Endoscopy, Fluorescence, Indocyanine green, Near-infrared

Operative Neurosurgery 17:32–42, 2019 DOI: 10.1093/ons/opy213

The endoscope was pioneered by rhinologists and advanced for use in skull-base tumor surgery with collaboration between neurosurgery and otorhinolaryngology.[1-6] Despite advances in tumor visualization, complete resection remains a challenge. Ventral skull-base tumors have suboptimal resection rates, with relatively high recurrence rates (>15-20% in pituitary adenomas, for instance).[7-14] One potential strategy to improve resection is fluorescence-guided surgery.

Recently, intraoperative fluorescence imaging has garnered interest. Five-aminolevulinic acid (5-ALA), for instance, is a visible light-spectrum contrast agent recently FDA approved for gliomas. 5-ALA has been shown to improve glioma resection rates and progression-free survival rates.[15-17] Despite its benefits, limitations include poor signal penetration, autofluorescence of normal parenchyma, and limited success in patients with ventral skull-base tumors.[18]

ABBREVIATIONS: 5-ALA, five-aminolevulinic acid; **EPR,** enhanced permeability and retention; **GLCM,** gray level co-occurrence matrix; **ICG,** indocyanine-green; **MRI,** magnetic resonance imaging; **NIR,** near-infrared; **NPV,** negative predictive value; **PPV,** positive predictive value; **ROI,** region of interest; **SBR,** signal-to-background ratio; **SWIG,** second-window ICG

Supplemental digital content is available for this article at www.operativeneurosurgery-online.com.

Indocyanine green (ICG) is a FDA-approved near-infrared (NIR) contrast agent that has traditionally been used for intraoperative video angiography by intravenous delivery shortly before visualization. In contrast, we have developed an alternative technique called the "second-window ICG (SWIG)."[19–22] Instead of a 5 to 25 mg bolus, we inject a systemic dose of 5 mg/kg approximately 24 h prior to surgery. Through the enhanced permeability and retention (EPR) effect, ICG accumulates within tumor tissues with permeable vasculature endothelium, thus allowing for tumor visualization 24 h after injection.[23]

We have applied the SWIG technique in gliomas, meningioma, and brain metastases using an NIR exoscope system, demonstrating excellent sensitivity.[20-22] In this study, we report early results and potential challenges associated with the application of this technique in endonasal endoscopic, ventral skull-base surgery. In addition, we hypothesized that preoperative gadolinium enhancement correlates with intraoperative NIR signal-to-background ratio (SBR), based on our prior results in craniectomies.[20-22]

METHODS

Study Design

Our institution's Institutional Review Board approved this study, and all patients gave informed consent. This study is registered under clinicaltrials.gov, and recruitment began June 2015. Patients over the age of 18 with ventral skull-base tumors planning to undergo endoscopic endonasal surgery were enrolled and analyzed. Main exclusion criteria were pregnancy and history of iodine allergy. All patients underwent preoperative magnetic resonance imaging (MRI) scan of the brain with intravenous gadolinium. All patients were made aware that the extent of surgery would not significantly change based on NIR findings and that biopsies would be taken only if considered safe by the senior surgeon.

ICG Administration

We intravenously injected our patients with 5 mg/kg dose of ICG (Akorn Pharmaceuticals, Decatur, Illinois; C43H47N2O6S2.Na) approximately 16 to 30 h prior to surgery, based on preclinical animal study results as well as our prior studies in intracranial tumors.[19] We found no immediate complications from ICG administration.

NIR Imaging Platform

All cases were recorded using the FDA-approved VisionSense Iridium™ (Visionsense, Philadelphia, Pennsylvania), a 4-mm endoscope NIR camera system that utilizes dual optics for simultaneously imaging visible light and NIR views in real time. When compared to other fluorescent visualization systems, VisionSense system demonstrated the highest sensitivity for NIR fluorescent dye over a wider range of concentrations.[24,25]

Operative Procedure

A uninostril or binostril endoscopic endonasal approach was performed in all cases. Otorhinolaryngologists performed the endonasal approach using the Storz™ (Tuttlingen, Germany) endoscope system.[26,27] For pituitary adenomas, the sellar face and floor were exposed, then the sella was opened using standard techniques. The dura was kept intact for as long as possible in order to visualize NIR signal through the dura. A larger bone opening–transtuberculum–was used for craniopharyngiomas, and a transclival approach was used for clival chordomas.

Upon encountering the tumor, the Visionsense Iridium™ was utilized to visualize the visible-light and NIR images (Figure 1). For intraoperative analysis of tumor NIR signal, the 2 modes were superimposed in real time on the video output (**Video**, **Supplemental Digital Content**). Tumor specimens were acquired and coded as consistent with tumor based on the senior surgeon's impression under white light (yes/no) and NIR fluorescence (yes/no). The histopathologic diagnoses of the specimens were later determined by the pathology department. After specimen collection, surgery continued in the standard-of-care manner without the guide of NIR fluorescence. When the senior neurosurgeon determined that a complete resection was achieved using white light visualization, NIR imaging was used to visualize the operative site. Any regions of residual fluorescence were biopsied, coded, and sent to pathology at the discretion of the senior surgeon.

NIR Excitation Light Illumination Profile Analysis

The endoscope distributes the excitatory laser in a nonuniform manner due to its smaller size and distance from tumor tissue.[19-22] In a dark room void of ambient visible and NIR light, we prepared a positive control sample by bathing a 3×3 cm square white paper in a 1.3 μM ICG solution for 5 s. We let the control paper dry for 60 s and imaged it 12 mm away from the endoscope using both white light and NIR, with the NIR detector sensitivity (ie, gain percent) set at 50%, which we have previously observed to provide strong NIR signal without significant background reflection/noise.

Imaging Analysis

Visionsense Iridium™ images were recorded and stored for analysis using the Visionsense Player software (VSPlayer v1.8.05.01). For each case, areas corresponding to the tumor site and normal tissue were identified and confirmed by the senior surgeon in 3 different still frames. Region of interest (ROI) encasing the 2 types of area within the same still was drawn, and the average pixel intensity value corresponding to each ROI was obtained using the ImageJ software (https://imagej.nih.gov/ij; NIH, Bethesda, Maryland) as a quantitative measure of fluorescence. The SBR was calculated by dividing the tumor site intensity by the adjacent background intensity. We previously demonstrated this method to have strong inter-rater correlation.[28]

Similarly, preoperative T1-weighted, gadolinium-enhanced MRI scans for each patient in at least 2 different views were used to calculate the ratio between the signal intensities of the tumor region and normal white matter (from here on, referred to as T1-to-normal).

Tumor Heterogeneity Analysis

The gray level co-occurrence matrix (GLCM) is a widely used technique for extracting second order statistical texture features, and it was used to analyze textural parameters of the tumor regions from the preoperative T1-weighted, gadolinium-enhanced MRI scans.[29]

Specifically, GLCM entropy was used to quantitatively analyze the randomness of intensity distribution as follows.

$$\text{Entropy} = -\sum_{i=0}^{G-1}\sum_{j=0}^{G-1} p(i,j) * \log(p(i,j))$$

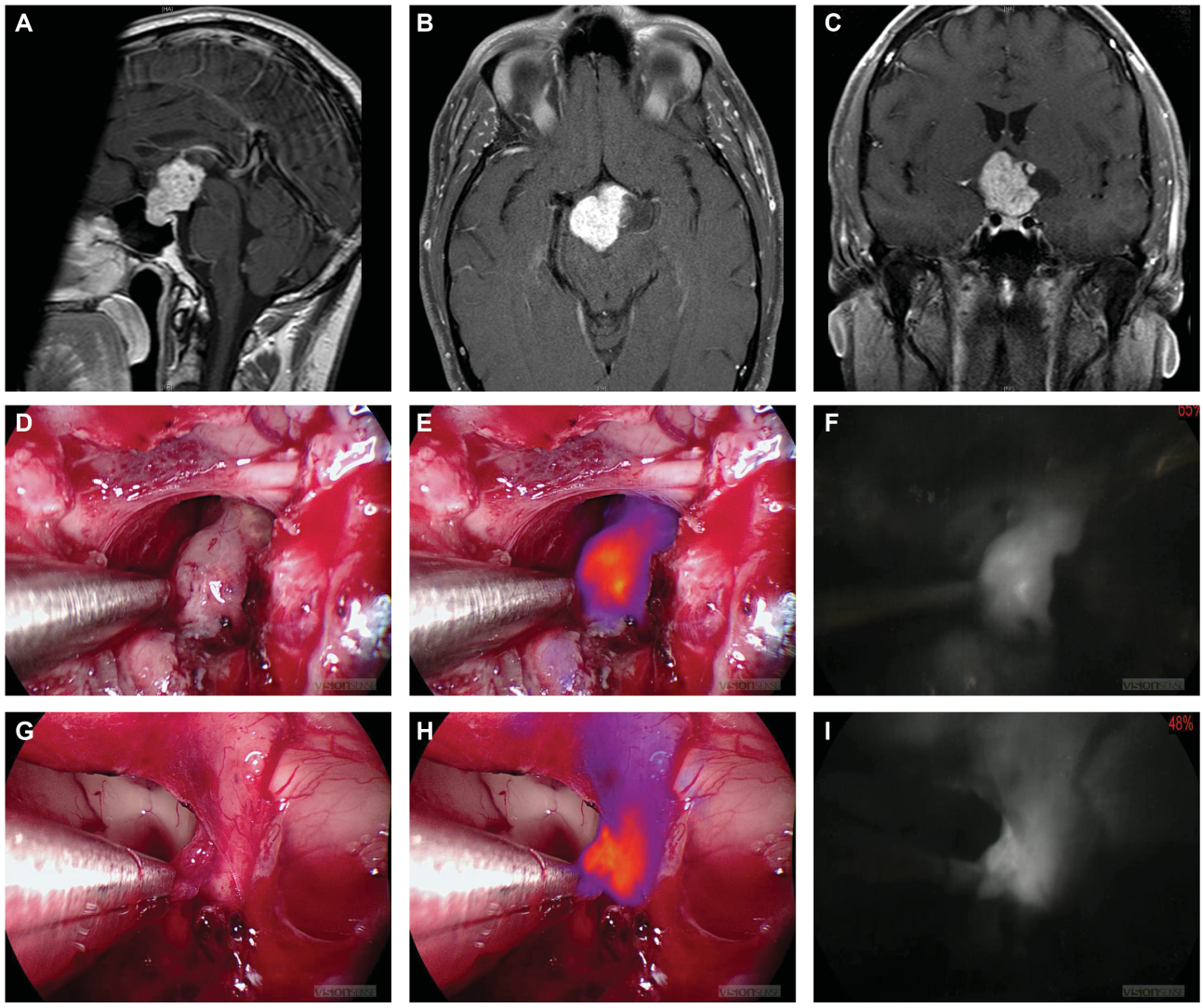

FIGURE 1. *Patient ID 509 with a craniopharyngioma.* **A-C**, *Preoperative T1-weighted, gadolinium-enhanced MRI scans.* **D-F**, *White light, NIR overlay, and NIR-only views, respectively, of the main tumor.* **G-I**, *White light, NIR overlay, and NIR-only views, respectively, of an NIR-positive margin in the third ventricle under the optic chiasm. Left hypothalamic wall was biopsied based on presence of strong NIR signal. The sample was later verified to be a tumor tissue.*

where G is the number of gray levels used. $p_x(i)$ is the ith entry in the marginal-probability matrix obtained by summing the rows of $p(i, j)$. The entropy value was used as a quantitative representation of tumor heterogeneity.[30,31]

Statistical Analysis

Statistical comparison with linear regression, t-tests, nonparametric tests were performed using Stata 10^{TM} (StataCorp LLC, College Station, Texas). Two-by-two contingency tables were constructed to calculate the sensitivity, specificity, positive predictive value (PPV), and negative predictive value (NPV).

RESULTS

Clinical Design

Between June 2015 and July 2017, 15 patients between the ages of 36 and 82 (mean age 53.8) with a presumed diagnosis of pituitary adenoma, chordoma, or craniopharyngioma were enrolled by the senior author (Table 1). Of the 15 patients, 8 (mean age 54) had pituitary adenomas, 3 (mean age 64) had craniopharyngiomas, and 4 (mean age 52) had chordomas. Two patients had prior surgery for pituitary adenomas and none had prior radiation therapy. All patients were deemed surgical candidates and consented to enroll in the SWIG study. All patients

TABLE 1. Summary of Patient and Tumor Characteristics

Tumor type	ID	Age	Sex	BMI	Clinical features at presentation	Prior treatment	Pathology
Pituitary adenoma	69	54	M	30.1	Acromegaly	–	Somatotroph adenoma
	82	67	F	18.5	Hemianopia; central hypothyroidism	–	Silent somatotroph adenoma
	98	59	M	35.9	Hemianopia; central hypogonadism; hypoadrenalism	–	Null cell
	105	40	F	28.4	Right facial numbness; headaches	–	Silent somatotroph adenoma
	116	69	M	32	Hypothyroidism; hypocortisolism	–	Null cell
	512	46	F	35.7	Cushing's disease; headaches	Surgery	Corticotroph adenoma
	515	40	F	29.8	Cushing's disease	–	Corticotroph adenoma
	516	57	M	27.3	Hypogonadotrophic hypogonadism; headaches	Surgery	Null cell
Craniopharyngioma	73	70	F	28.8	Hemianopia; blurred vision; migraines; hypopituitarism	–	Adamantinomatous type, WHO grade I
	76	82	F	26.9	Diplopia; hemianopia; dizziness;	–	Adamantinomatous type, WHO grade I
	509	40	M	33.5	Bitemporal hemianopia; hypogonadism; headaches	–	Adamantinomatous type, WHO grade I
Chordoma	13	45	M	36.4	Sixth nerve palsy; diplopia; headaches	–	Chordoma
	83	76	F	30.3	Sixth nerve palsy; diplopia	–	Chordoma
	84	49	F	35.5	Left hemiparesis	–	Chordoma
	103	40	F	35.4	Right diplopia; headaches	–	Chordoma

BMI, body mass index; ID, study number; WHO, World Health Organization.

tolerated 5 mg/kg intravenous ICG injection administered 16 to 30 h prior to surgery without any adverse events.

Endoscope NIR Demonstrates Greater Vignetting than White Light

Prior to using the NIR endoscope camera system for tumor identification, we evaluated the endoscope's light distribution pattern. We found that white light demonstrated mild vignetting, or reduced peripheral light intensities compared to the center. In contrast, the NIR view showed a higher degree of vignetting (Figure 2A). The intensity profile was plotted for both white light and NIR view (Figures 2B and 2C). The intensity distribution pattern of the white light view (Figure 2D, black line) had a broader profile toward the center (Kurtosis = 1.96), while that of the NIR view (Figure 2D, blue line) demonstrated a peaked pattern toward the center of the curve with a relatively higher kurtosis (Kurtosis = 2.40).

NIR Tumor Fluorescence Varies Based on Tumor Type and MRI Gadolinium Enhancement

All pituitary adenomas demonstrated NIR signal with an average SBR of 3.9 ± 0.8 (range 3.14-5.55; Figure 3). All craniopharyngiomas also demonstrated NIR signal with an average SBR of 4.1 ± 1.7 (range 1.88-6.06), which was not statistically distinct from that of pituitary adenomas (Wilcoxon rank sum, $P = .78$; Figure 4). Chordomas had an average SBR of 2.1 ± 0.6 (range 1.20-3.52), which was statistically weaker than patients with pituitary adenomas (Wilcoxon rank sum, $P = .048$).

To understand the difference in NIR signal in these tumor types, we examined multiple variables: tumor size, T1-to-normal ratio, GLCM entropy, gender, BMI, time from injection to visualization, and tumor pathology (Table 2). Using univariate linear regression to screen and predict SBR, we identified tumor pathology, T1-to-normal, and gender as 3 variables with a P-value $< .2$. Prediction of SBR was performed using multivariate analysis, and the best predictor was T1-to-normal ratio ($P = .0003$). If T1-to-normal increases by 1 point (ie, there is stronger contrast enhancement on T1 MRI), then the NIR SBR increases by 2.17 (Figure 5A).

We plotted T1-to-normal against the corresponding SBR for pituitary adenomas (Figure 5B). Using linear regression, we found that for every 1-point increase in T1-to-normal, the SBR increased by 1.53 ($R^2 = .52$). For craniopharyngiomas, every 1-point increase in T1-to-normal corresponded to an SBR increase of 3.04 ($R^2 = 0.82$; Figure 5C). For chordomas, each 1-point increase in T1-to-normal led to an SBR increase of 6.02 ($R^2 = 0.97$; Figure 5D).

SWIG is Sensitive But not Specific for Residual Pituitary Adenoma

Fifteen specimens (8 bulk tumor and 7 margin biopsies) were analyzed for patients with pituitary adenomas. Of the 15 specimens, 10 (66.7%) demonstrated adenoma tissue on final histopathology and all 15 were positive for NIR signal. The final histopathological report of tumor specimens as the gold standard was compared to the surgeon's impression under white light. We calculated the sensitivity, specificity, PPV, and NPV, which were 90%, 100%, 100%, and 83%, respectively. In contrast, the sensitivity, specificity, PPV, and NPV of NIR intraoperative imaging for identifying tumor were 100%, 20%, 71%, and 100%, respectively (Table 3).

Given the rate of low sensitivity of pituitary identification with NIR imaging, we assessed the effects of the automatic sensor gain adjustment feature inherent in the VisionSense camera software, which could have contributed to some of the false identification of tumor tissues based on fluorescence. We found that true positive samples from the NIR view had a lower average IR gain-percent (76%) setting compared to that of false positive samples (97.5%; Wilcoxon rank sum, $P < .05$), suggesting that the NIR sensor's

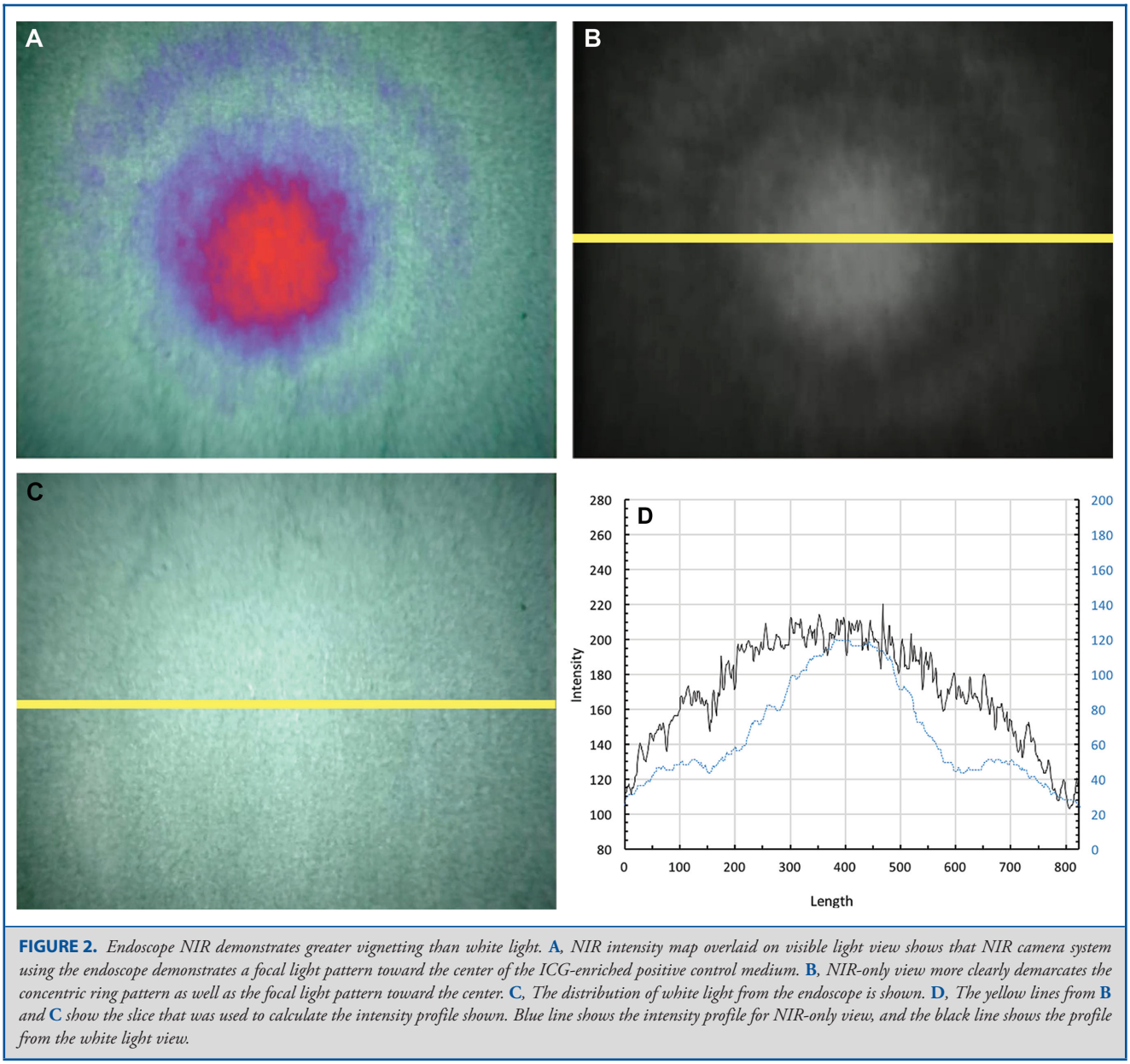

FIGURE 2. *Endoscope NIR demonstrates greater vignetting than white light.* **A**, *NIR intensity map overlaid on visible light view shows that NIR camera system using the endoscope demonstrates a focal light pattern toward the center of the ICG-enriched positive control medium.* **B**, *NIR-only view more clearly demarcates the concentric ring pattern as well as the focal light pattern toward the center.* **C**, *The distribution of white light from the endoscope is shown.* **D**, *The yellow lines from* **B** *and* **C** *show the slice that was used to calculate the intensity profile shown. Blue line shows the intensity profile for NIR-only view, and the black line shows the profile from the white light view.*

sensitivity was increased to the point of causing false-positive signal readings.

Four specimens (4 bulk tumor specimens and no additional margin biopsies) were analyzed from patients with chordomas, and 5 specimens (3 bulk tumor specimens and 2 additional margin biopsies) were analyzed from patients with craniopharyngiomas. All specimens were positive for NIR signal and demonstrated tumor tissue based on final histopathology. Due to the limited number of specimens for chordomas and craniopharyngiomas, accurate values for sensitivity, specificity, PPV, and NPV could not be calculated.

DISCUSSION

Fluorescent contrast agents provide a novel approach to visualizing tumors, detecting margins, and assessing extent of resection.[32] Although 5-ALA, a visible-light fluorophore, is FDA approved for use in glioma resection, its use is limited in pituitary adenomas, craniopharyngiomas, or chordomas due to poor tissue uptake and visualization.[18,33,34] In contrast, ICG is an FDA-approved NIR fluorophore, with tissue-penetrating fluorescence and minimal autofluorescence from surrounding tissue.

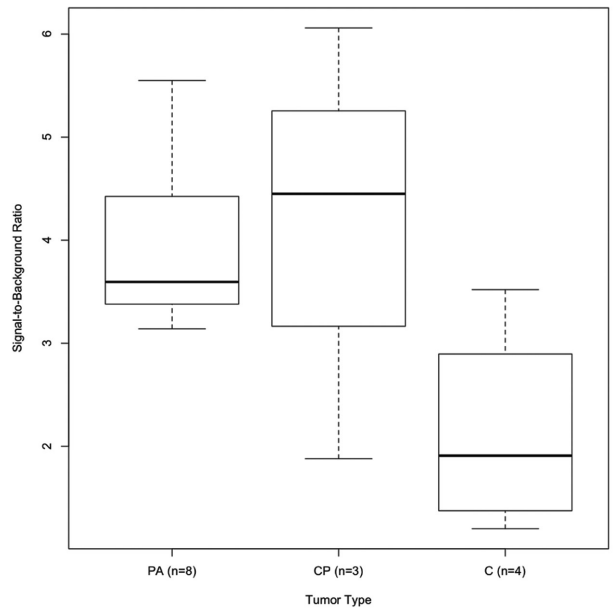

FIGURE 3. *NIR tumor fluorescence varies based on tumor type. All 8 pituitary adenomas demonstrated NIR positivity and fluoresced with an average SBR of 3.9 ± 0.8. Craniopharyngiomas (CP) had the highest average SBR of 4.1 ± 1.7, which was not statistically different from the average SBR of pituitary adenomas (PA; Wilcoxon rank sum, P = .78). However, the average SBRs of both pituitary adenomas and cranoipharyngiomas were statistically distinct from that of chordomas (C; SBR = 2.1 ± 0.6).*

SWIG has been shown in our prior papers to accumulate extensively in gadolinium-enhancing gliomas, meningiomas, and brain metastases.[20-22] Thus, we hypothesized that ICG could also accumulate in pituitary adenomas, craniopharyngiomas, and chordomas, as most demonstrate contrast enhancement on T1-MRI. Using intraoperative NIR fluorescence imaging, we were able to demonstrate strong fluorescence in tumor specimens with increased sensitivity compared to endoscopy alone. We believe that the high sensitivity of NIR imaging for tumor detection and its correlation with gadolinium enhancement may provide clinical benefit.

Rationale for NIR Imaging in Endoscopy

Complete resection of pituitary adenomas, chordomas, and craniopharyngiomas can be curative, but is often not achieved despite best attempts by the surgeon. One potential factor that reduces effective resection is the <100% sensitivity of the surgeon in detecting neoplastic tissue using endoscopy alone. In our study, as well as in our previous publications, the sensitivity for visible light only is approximately 90% while the specificity is >90 to 95%.[20-22] Thus, some areas of tumor can be missed during surgery, leading to subtotal resection. NIR imaging with SWIG, on the other hand, demonstrates 100% sensitivity, although at the cost of reduced specificity. By combining the exquisitely high sensitivity of SWIG with the near 100% specificity of the trained neurosurgeon's eyes, surgeons can detect previously missed areas of tumor, resulting in increased gross total resection rates while minimizing iatrogenic damage to surrounding benign tissue.

NIR Camera and the Endoscopic System

In contrast to the VisionSense exoscope used in open craniotomies, the endoscope features a smaller excitation laser field and smaller angle of view which can limit fluorophore visualization. Based on our control experiments, we believe that the narrow profile of the endoscope limits more thorough spread of the excitation laser from the tip of the endoscope, thus increasing the relative focus of NIR excitation and emission toward the center of the view compared to the periphery.

This uneven distribution of the NIR signal detection has the potential to overestimate fluorescence intensity if the potential area of tumor is observed toward the center of the view while the background is located in the less-illuminated periphery. Since such illumination profile is inherent to the system itself and not modifiable by the operator, it is important to consider different techniques to make NIR measurements consistent across different samples. In our study, we consistently sampled still frames with the tumor in the center of the view in order to keep the SBR inflation consistent across every sample. We believe that in order to increase interstudy comparability, the endoscope system itself must be able to produce a more homogenous illumination profile. While this study was conducted using the VisionSense system due to its demonstrated high sensitivity, other NIR-capable endoscopes exist and have been used in other fields of surgery. Thus, NIR imaging is easily accessible to neurosurgeons globally.

NIR Signal Based on Tumor Types

While tumor size did not correlate with SBR, we observed lower SBR for tumors with a more heterogeneous architecture based on T1-MRI gadolinium-enhancement profile. Chordomas demonstrated the lowest average NIR signal and the most architectural heterogeneity as measured using both GLCM entropy analysis and visual inspection (Figure 6). Among many potential variables, we postulate that the differences in ICG uptake between each tumor type is the most relevant factor for this observation. For example, the relative abundance of pockets of necrosis and limited vasculature demonstrated in chordomas may have limited ICG uptake and therefore produced a lower average NIR signal. While our analysis between tumor heterogeneity and SBR did not yield statistically significant results, we believe this is secondary to low sample size. A future study with larger sample sizes encompassing tumors across a wider variety of homogeneity would further demonstrate whether this finding is relevant.

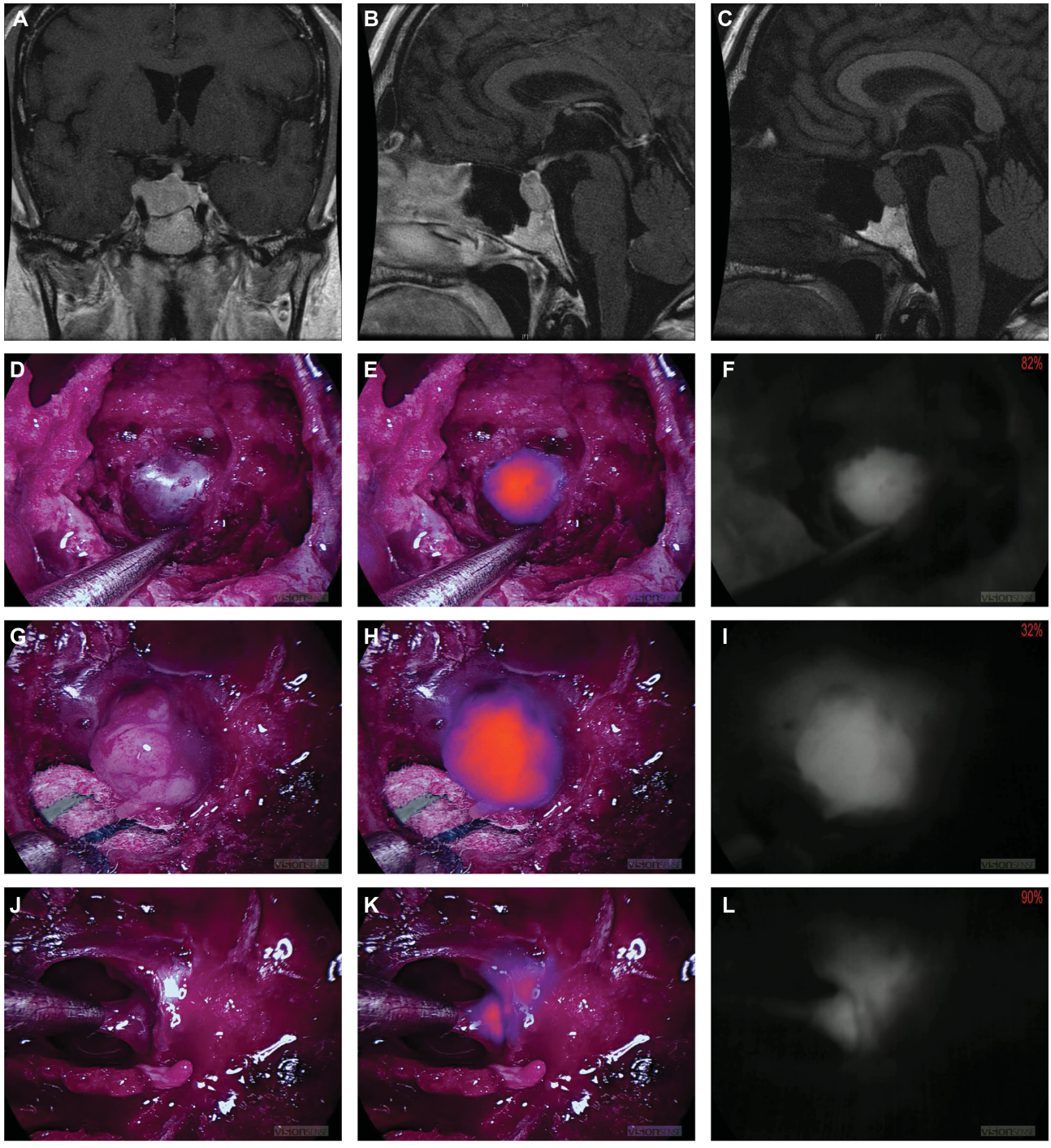

FIGURE 4. *Patient ID 116 with a pituitary adenoma.* **A** *and* **B**, *Preoperative T1-weighted, gadolinium-enhanced MRI scans.* **C**, *Preoperative T1-weighted MRI scan without gadolinium-enhancement.* **D-F**, *White light, NIR overlay, and NIR-only views, respectively, of the tumor region before dura removal.* **G-I**, *White light, NIR overlay, and NIR-only views, respectively, of the fully exposed and isolated tumor tissue.* **J-L**, *White light, NIR overlay, and NIR-only views, respectively, of a margin specimen detected by the NIR signal after primary debulking.*

TABLE 2. Near-Infrared Signal to Background Ratio of Primary Tumor Specimen

Tumor type	ID	Max tumor diameter on pre-op MRI (mm)	SBR	T1-TO-normal	GLCM entropy	Time from ICG injection to camera visualization (h)
Pituitary adenoma	69	9.84	3.72	30.1	5.53	16.8
	82	39.4	3.32	18.5	5.62	19.6
	98	52.4	4.22	35.9	5.02	21.2
	105	41.8	3.14	28.4	7.40	18.8
	116	23.8	5.55	32.0	6.72	16.2
	512	15.0	3.44	35.7	6.26	25.3
	515	16.3	4.63	29.8	6.73	24.0
	516	20.9	3.47	27.3	4.69	15.5
Mean ± SD		27 ± 15	3.9 ± 0.8	1.6 ± 0.4	6.0 ± 0.9	20 ± 4
Craniopharyngioma	73	24.0	1.88	28.8	6.47	28.1
	76	17.5	4.45	26.9	7.04	25.8
	509	35.5	6.06	33.5	7.05	29.1
Mean ± SD		26 ± 9	4.13 ± 2	1.7 ± 0.6	6.9 ± 0.3	28 ± 2
Chordoma	13	26.5	2.27	36.4	7.64	25.1
	83	45.9	3.52	30.3	7.48	22.3
	84	32.8	1.55	35.5	6.27	23.7
	103	10.7	1.20	35.4	6.60	30.0
Mean ± SD		29 ± 15	2.1 ± 1	1.2 ± 0.2	7.0 ± 0.7	25 ± 3

GLCM, gray level co-occurrence matrix; ICG, Indocyanine green; ID, study number; MRI, magnetic resonance imaging; SBR, signal-to-background ratio; SD, standard deviation.

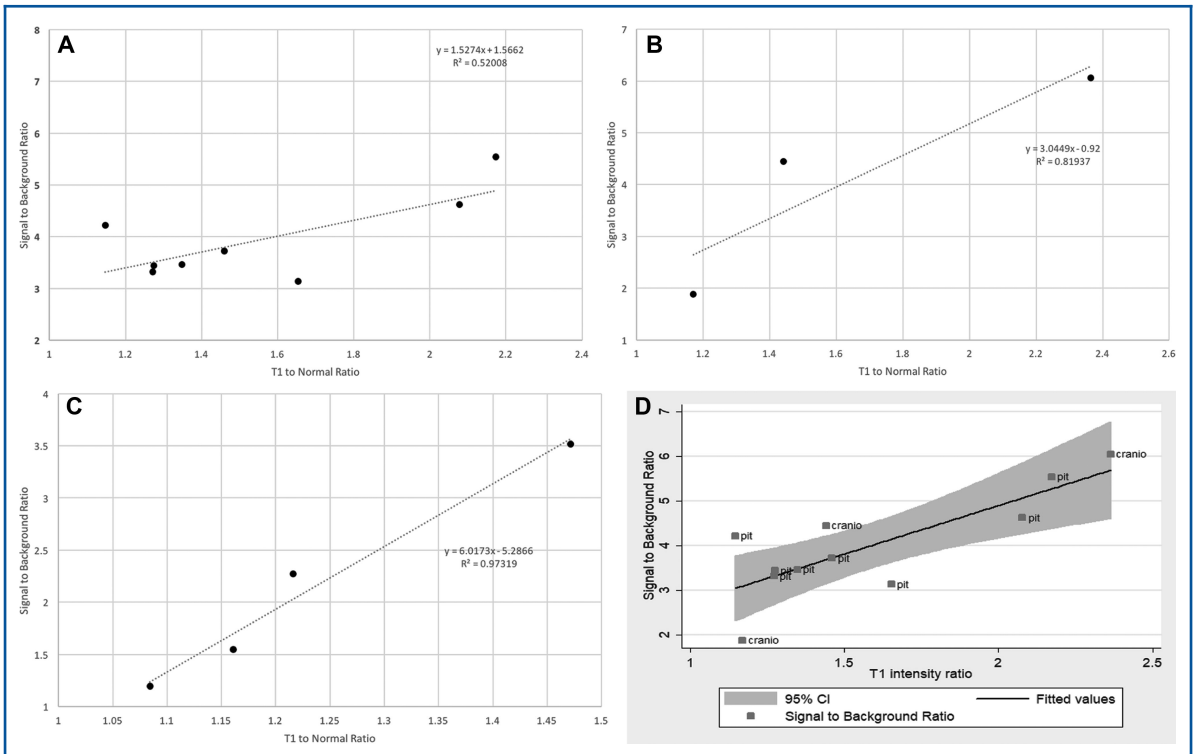

FIGURE 5. *NIR signal is correlated with gadolinium enhancement by MRI.* **A**, *T1-to-normal ratio vs SBR for all pituitary adenomas and craniopharyngiomas combined with 95% confidence interval.* **B**, *T1-to-normal ratio vs SBR for pituitary adenomas.* **C**, *T1-to-normal ratio vs SBR for cranoipharyngiomas.* **D**, *T1-to-normal ratio for chordomas.*

TABLE 3. Test Characteristics of White Light vs NIR View in 8 Pituitary Adenoma Patients (15 Specimens)

		Test characteristics of white light in 15 pituitary adenoma specimens					
		Positive for tumor under white light, according to surgeon		Sensitivity (95% CI)	Specificity (95% CI)	PPV (95% CI)	NPV (95% CI)
		Yes	No				
Tumor pathology according to ultimate pathological diagnosis	Yes	9	0	90%	100%	100%	83%
	No	1	5				
		Test characteristics of NIR in 15 pituitary adenoma specimens					
		Positive for tumor under NIR endoscope, according to surgeon		Sensitivity (95% CI)	Specificity (95% CI)	PPV (95% CI)	NPV (95% CI)
		Yes	No				
Tumor pathology according to ultimate pathological diagnosis	Yes	10	4	100%	20%	71%	100%
	No	0	1				

CI, confidence interval; NIR, near-infrared; NPV, negative predictive value; PPV, positive predictive value.

Gadolinium Enhancement and NIR Signal

We hypothesized that SWIG as an intraoperative tumor imaging adjunct may be useful for initial localization of contrast-enhancing tumors based on our previous observations in other intracranial tumors. Indeed, as seen in Figure 5, the T1-to-normal ratio appears to linearly correlate with the NIR signal, implying that the amount of gadolinium accumulation in a tumor correlates with the accumulation of ICG within the tumor. Although the mechanism of gadolinium enhancement in tumors does not rely on the EPR effect, gadolinium localizes to areas of vascular permeability and blood-brain barrier breakdown. Similarly, SWIG is believed to accumulate in tumor tissue with permeable vasculature via the EPR effect. Thus, the correlation between SWIG signal and gadolinium enhancement is sensible, and the presence of enhancement could guide surgeons toward appropriate selection of patients for intraoperative SWIG usage.

Limitations

Our study is limited by its small sample size (15 cases) encompassing 3 different tumor types. Thus, while we were able to gather suggestive data, we were unable to make statistically meaningful conclusions. However, as the main objective of this study was to evaluate the feasibility of using NIR imaging in endoscopy, the small amount of data generated in this study will serve to launch future studies.

Secondly, the SBR is an arbitrary ratio as it is not an absolute measure of fluorescence, but rather a relative measure of fluorescence in the area of interest versus the surrounding area. Thus, calculations can vary by a small amount at each repetition and can be subject to bias if calculated by one person. However, we demonstrated in a previous study that the inter-rater correlation was very high for SBR to try to minimize this bias.

Future Direction

The mechanism of ICG accumulation is not specific for tumor cells, and at high doses, it can bind to plasma albumin and remain trapped within the extracellular matrix through the EPR effect. Furthermore, enhanced vascular permeability is not unique to tumor, as it can be caused by inflammation, necrosis, etc. This likely explains SWIG's low specificity. To improve upon NIR-imaging specificity, we suggest the development of targeted dyes. Indeed, we have demonstrated that a novel dye composed of ICG conjugated to folate can specifically target folate-receptor-overexpressing pituitary adenomas with near 100% sensitivity and specificity.[35,36] Thus, development of novel targeted dyes for other tumor types could greatly improve the neurosurgeons' tumor-detecting abilities to ultimately improve patient outcome.

CONCLUSION

In this paper, we demonstrate that SWIG (a systemic dose of ICG) can provide effective intraoperative NIR optical contrast during endoscopic endonasal surgery of ventral skull-base lesions. While the utility of ICG is promising due to enhanced sensitivity for residual tumor detection, it is limited by low specificity. Overall, we believe that intraoperative NIR imaging during endoscopy has the potential to enhance surgical resection rates and improve patient outcome.

Disclosures

Supported in part by the National Center for Advancing Translational Sciences of the National Institutes of Health (UL1TR001878), and the Institute for

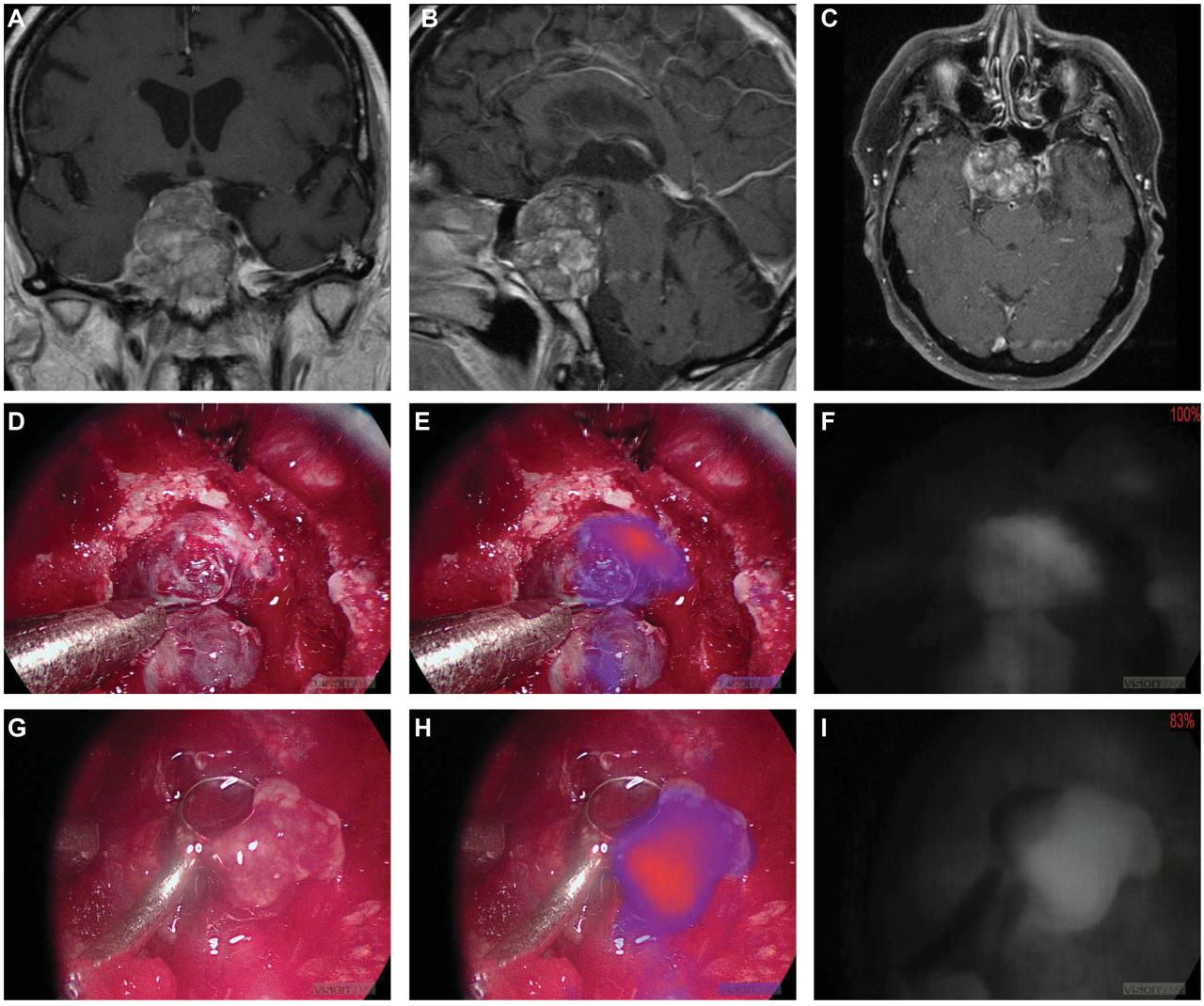

FIGURE 6. *Patient ID 83 with a chordoma.* **A-C**, *Preoperative T1-weighted, gadolinium-enhanced MRI scans.* **D-F**, *White light, NIR overlay, and NIR-only views, respectively, of the tumor region before dura removal.* **G-I**, *White light, NIR overlay, and NIR-only views, respectively, of the fully exposed and isolated main tumor tissue.*

Translational Medicine and Therapeutics of the University of Pennsylvania. The content is solely the responsibility of the authors and does not necessarily represent the official views of the NIH. Dr Lee owns stock options in VisionSense. Dr Singhal holds patent rights over technologies presented in this article. The other authors have no personal, financial, or institutional interest in any of the drugs, materials, or devices described in this article.

REFERENCES

1. Kennedy DW, Zinreich SJ, Rosenbaum AE, Johns ME. Functional endoscopic sinus surgery: Theory and diagnostic evaluation. *Arch Otolaryngol Head Neck Surg*. 1985;111(9):576-582.
2. Carrau RL, Jho HD, Ko Y. Transnasal-transsphenoidal endoscopic surgery of the pituitary gland. *Laryngoscope*. 1996;106(7):914-918.
3. Jho HD, Carrau RL. Endoscopy assisted transsphenoidal surgery for pituitary adenoma. *Acta Neurochir*. 1996;138(12):1416-1425.
4. Zwagerman NT, Zenonos G, Lieber S, et al. Endoscopic transnasal skull base surgery: pushing the boundaries. *J Neurooncol*. 2016;130(2):319-330.
5. Adappa ND, Lee JYK, Chiu AG, Palmer JN. Olfactory groove meningioma. *Otolaryngol Clin North Am*. 2011;44(4):965-980.
6. Ali ZS, Lang SS, Kamat AR, et al. Suprasellar pediatric craniopharyngioma resection via endonasal endoscopic approach. *Childs Nerv Syst*. 2013;29(11):2065-2070.
7. Losa M, Mortini P, Barzaghi R, et al. Early results of surgery in patients with nonfunctioning pituitary adenoma and analysis of the risk of tumor recurrence. *J Neurosurg*. 2008;108(3):525-532.
8. Thawani J, Ramayya A, Pisapia J, Abdullah K, Lee J, Grady M. Operative strategies to minimize complications following resection of pituitary macroadenomas. *J Neurol Surg B*. 2016;78(02):184-190.

9. Karavitaki N, Cudlip S, Adams CBT, Wass JAH. Craniopharyngiomas. *Endocr Rev*. 2006;27(4):371-397.
10. Yang I, Sughrue ME, Rutkowski MJ, et al. Craniopharyngioma: A comparison of tumor control with various treatment strategies. *Neurosurg Focus*. 2010;28(4):E5.
11. Al-Mefty O, Kadri PAS, Hasan DM, Isolan GR, Pravdenkova S. Anterior clivectomy: surgical technique and clinical applications. *J Neurosurg*. 2008;109(5):783-793.
12. Colli BO, Al-Mefty O. Chordomas of the skull base: follow-up review and prognostic factors. *Neurosurg Focus*. 2001;10(3):1-11.
13. Sen C, Triana A. Cranial chordomas: results of radical excision. *Neurosurg Focus*. 2001;10(3):1-7.
14. Sekhar LN, Pranatartiharan R, Chanda A, Wright DC. Chordomas and chondrosarcomas of the skull base: results and complications of surgical management. *Neurosurg Focus*. 2001;10(3):1-4.
15. Zhao S, Wu J, Wang C, et al. Intraoperative fluorescence-guided resection of high-grade malignant gliomas using 5-aminolevulinic acid-induced porphyrins: a systematic review and meta-analysis of prospective studies. *PLoS One*. 2013;8(5):e63682.
16. Stummer W, Pichlmeier U, Meinel T, Wiestler OD, Zanella F, Reulen HJ. Fluorescence-guided surgery with 5-aminolevulinic acid for resection of malignant glioma: a randomised controlled multicentre phase III trial. *Lancet Oncol*. 2006;7(5):392-401.
17. Stummer W, Novotny A, Stepp H, Goetz C, Bise K, Reulen HJ. Fluorescence-guided resection of glioblastoma multiforme utilizing 5-ALA-induced porphyrins: a prospective study in 52 consecutive patients. *J Neurosurg*. 2000;93(6):1003-1013.
18. Eljamel MS, Leese G, Moseley H. Intraoperative optical identification of pituitary adenomas. *J Neurooncol*. 2009;92(3):417-421.
19. Zeh R, Sheikh S, Xia L, et al. The second window ICG technique demonstrates a broad plateau period for near infrared fluorescence tumor contrast in glioblastoma. *PLoS One*. 2017;12(7):e0182034.
20. Lee JYK, Pierce JT, Thawani JP, et al. Near-infrared fluorescent image-guided surgery for intracranial meningioma. *J Neurosurg*. 2017;128(2):1-11.
21. Lee JYK, Thawani JP, Pierce J, et al. Intraoperative near-infrared optical imaging can localize gadolinium-enhancing gliomas during surgery. *Neurosurgery*. 2016;79(6):856-871.
22. Maeda H, Wu J, Sawa T, Matsumura Y, Hori K. Tumor vascular permeability and the EPR effect in macromolecular therapeutics: a review. *J Control Release*. 2000;65(1-2):271-284.
23. Lee JYK, Pierce JT, Zeh R, et al. Intraoperative near-infrared optical contrast can localize brain metastases. *World Neurosurg*. 2017;106:120-130.
24. Cho SS, Zeh R, Pierce JT, Salinas R, Singhal S, Lee JYK. Comparison of near-infrared imaging camera systems for intracranial tumor detection. *Mol Imaging Biol*. 2018;20(2):213-220.
25. DSouza AV, Lin H, Henderson ER, Samkoe KS, Pogue BW. Review of fluorescence guided surgery systems: identification of key performance capabilities beyond indocyanine green imaging. *J Biomed Opt*. 2016;21(8):080901.
26. O'Malley BW, Grady MS, Gabel BC, et al. Comparison of endoscopic and microscopic removal of pituitary adenomas: single-surgeon experience and the learning curve. *Neurosurg Focus*. 2008;25(6):E10.
27. Elhadi AM, Hardesty DA, Zaidi HA, et al. Evaluation of surgical freedom for microscopic and endoscopic transsphenoidal approaches to the sella. *Neurosurgery*. 2015;11(Suppl 2):69-78.
28. Cho S, Zeh R, John P, et al. Folate receptor near-infrared optical imaging provides sensitive and specific intraoperative visualization of nonfunctional pituitary adenomas. *Oper Neurosurg Hagerstown*. In Press.
29. Ryu YJ, Choi SH, Park SJ, Yun TJ, Kim JH, Sohn CH. Glioma: Application of whole-tumor texture analysis of diffusion-weighted imaging for the evaluation of tumor heterogeneity. *PLoS One*. 2014;9(9):e108335.
30. Ganeshan B, Skogen K, Pressney I, Coutroubis D, Miles K. Tumour heterogeneity in oesophageal cancer assessed by CT texture analysis: preliminary evidence of an association with tumour metabolism, stage, and survival. *Clin Radiol*. 2012;67(2):157-164.
31. Haralick RM, Shanmugam K, Dinstein I. Textural features for image classification. *IEEE Trans Syst Man, Cybern*. 1973;SMC-3(6):610-621.
32. Zhang RR, Schroeder AB, Grudzinski JJ, et al. Beyond the margins: real-time detection of cancer using targeted fluorophores. *Nat Rev Clin Oncol*. 2017;14(6):347-364.
33. Zhao S, Wu J, Wang C, et al. Intraoperative fluorescence-guided resection of high-grade malignant gliomas using 5-aminolevulinic acid-induced porphyrins: A systematic review and meta-analysis of prospective studies. *PLoS One*. 2013;8(5):e63682.
34. Valdés PA, Leblond F, Kim A, et al. Quantitative fluorescence in intracranial tumor: implications for ALA-induced PpIX as an intraoperative biomarker. *J Neurosurg*. 2011;115(1):11-17.
35. Lee JYK, Cho SS, Zeh R, et al. Folate receptor overexpression can be visualized in real time during pituitary adenoma endoscopic transsphenoidal surgery with near-infrared imaging. *J Neurosurg*. 2017;25:1-14.
36. Evans CO, Yao C, Laborde D, Oyesiku NM. Folate receptor expression in pituitary adenomas cellular and molecular analysis. *Vitam Horm*. 2008;79:235-266.

Supplemental digital content *is available for this article at www.operativeneurosurgery-online.com.*

Supplemental Digital Content. Video. Superimposed view of NIR signal during surgery.

COMMENT

The authors describe the value of second window ICG in endoscopic endonasal ventral skull base surgery. The ICG is believed to accumulate within tumor tissue via the enhanced-permeability-and-retention (EPR) effect.

They conclude, in a series of 15 patients (8 adenoma, 3 craniopharyngioma, and 4 chordoma), that this technique can provide strong NIR optical tumor contrast of adenomas and craniopharyngiomas. Chordomas demonstrate the weakest signal, thus limiting its utility. Both nonfunctional and functional pituitary adenomas appear to accumulate dye, but utility for margin detection for the adenomas is limited by low specificity, which is a major limitation as it can result in unnecessary additional resection with potential complications. Craniopharyngiomas on the other hand appear to be a particularly promising target given the clean brain parenchyma background and strong SBR. However, the specificity remains low and also, it is relatively easy to distinguish craniopharyngioma from normal neural structures.

The technology is novel and promising, however it needs to be improved. It will be most important for fibrotic pituitary tumors where the distinction between the tumor and parenchyma is sometimes difficult. This small study can not show this particular utility. Hopefully the authors provide their larger series with more robust analyses in the future further exploring and confirming the usefulness of second window ICG in endoscopic endonasal surgery.

Amir R. Dehdashti
Manhasset, New York